Screen-Printed Fe_2O_3/ZnO thick films for gas sensing applications

K. Arshak*, I. Gaidan and L. Cavanagh
Microelectronic and Semiconductor Research Group, ECE Department,
University of Limerick,
National Technological Park, Limerick, Ireland.
Tel +353-61-202267.Fax: +353-61-338176
E-mail: khalil.arshak@ul.ie.
*-Corresponding author

Abstract

This paper investigates iron-oxide and zinc-oxide thick-films for gas sensing applications. The films were printed onto glass substrates with silver electrodes. The effects of propanol, methanol and ethanol vapor on the devices at room temperature (in the concentration range 500-2000ppm) were investigated. The percentage relative resistance change, $\Delta R = ((R_{gas} - R_{air})/R_{air})$ x100, was seen to increase linearly with increasing gas vapor concentration. The sensitivity of the films to the gas vapor was determined from the slope of the graphs. It was observed that various film compositions showed a higher sensitivity to propanol than to methanol and ethanol. Moreover, the sensitivity to propanol increased from 0.077 to 0.166 to 0.173%/ppm for the three samples with molecular weight composition ratios of: 90%/10%, 80/20% and 70%/30% of Fe_2O_3 to ZnO respectively. The response times of sensors 1, 2 and 3 (to 1000ppm step changes in propanol concentration) were 48.6 seconds, 86.4 seconds and 76.5 seconds, while the recovery times were 117 seconds, 186 seconds and 153 seconds respectively.

Keywords

Iron-oxide, zinc-oxide, alcohol vapor, gas sensor, thick-film

1. INTRODUCTION

The ever-increasing concern about the state of our environment has led many scientists to investigate methods that can detect and sense gases that have undesirable attributes. Gas sensors based on metal-oxides are playing an important role in the detection of toxic pollutants and the control of industrial processes [1]. It has long been known that the electrical properties of semiconductor materials change as a result of adsorption and/or reaction with gases in the atmosphere. This property of semiconductor materials is typically exploited for sensor development [2]. Numerous materials have been reported to be usable as metal oxide sensors including single-component (ZnO [3] , TiO_2 [4], and Fe_2O_3) [5] and multi-component ($SrFeO_3$ [6], $ZnFe_2O_4$ [7], and $SmCoO_3$ [8]) oxides. The single or multi-component oxide used depends on the properties of the materials and the gas sensing requirements. Titanium dioxide has been used as a thin film gas sensor to detect propanol (at 2100ppm concentrations), methanol (at 2600ppm concentrations) and ethanol (at 2600ppm concentrations) [9]. Iron-oxide and zinc-oxide has been used to detect CO and NO_2 in a thin film gas sensor that was prepared by liquid phase deposition (LPD)[5]. $SrFeO_3$ has been used as a sensing material to detect alcohol prepared by solid-state reaction technology proving most sensitive to ethanol vapor [6].

Devices can also be made to display degrees of selectivity via careful selection of materials and/or various pre-treatment methods. Selectivity proves to be a highly desirable characteristic in cases where sensors are required to perform in an environment that may contain interfering gases. Thick films based on zinc lanthanum and palladium oxide semiconductors were used to detect ethanol vapor [10], the sensor exhibited a higher sensitivity towards ethanol in comparison to liquid petroleum gas (LPG), carbon monoxide (CO) and hydrogen (H_2) [10]. While thick films of $SmFeO_3$ showed a much higher sensitivity to carbon monoxide (CO) in comparison to nitrogen dioxide (NO_2) [11].

Most oxide sensors require a heating element, which is generally printed on the back of the sensor to provide the elevated temperatures in which these devices typically operate (100 - 650˚C) [12]. This not only increases the power consumption of the device but also adds to the fabrication cost and complexity. Hence, the development of selective alcohol sensors, which can operate at lower temperatures, is the focus of much recent research [13].

This paper investigates the effects of propanol, methanol and ethanol vapor on a screen-printed polymer thick film gas sensor (consisting of iron-oxide and zinc-oxide)

operating at room temperature has been studied.

2. THICK-FILM TECHNOLOGY

Screen-printing drew its inspiration from an ancient Chinese printing technique for the decoration of pottery. The deposition process for a thick film device is essentially the same as that used for traditional silkscreen printing, with the major differences being the screen materials and the complexity of the printing machine. A thick film circuit is generally considered to be one created from layers of pastes deposited onto an insulating substrate [14].

The continued advancement of thick film methods resulted in more stable resistor pastes with wider resistively ranges and improved temperature coefficients [15]. The development of fine line screen printing methods along with improvements in dielectric materials for thick film capacitors and crossovers allowed for greatly increased component density, quality and cost effectiveness of thick film hybrid circuits.

The production of gas sensing layers by screen-printing technology has met the interest of the scientists working in the field. Screen-printing is a simple and automated manufacturing technique that allows the production of low-cost and robust sensors with good reproducibility [8, 16, 17], this in addition to the use of cheaper sensing materials and electrodes, allows the production of low cost gas sensors which meet the requirements of devices for industrial instrumentation. Thick film gas sensors based on semiconductor oxides and manufactured by screen-printing technology have certain advantages compared to many types of gas sensors [8, 17, 18], some of these advantages include: low cost, small size, ease of operation and manufacture.

2.1 Paste preparation

This section outlines the basic procedure for the preparation of a thick film paste. To produce thick film paste formulations, particles in microns ranges are required for the functional and vehicle systems respectively. In general, commercially available materials must firstly be ground down. The grinding process is best carried out at low speeds, because high rotation speed can cause the composite material to be embedded on the sides of the container, thus removing itself from the grinding media. After grinding, the particle size should be checked by using a suitable mesh to filter out and large particles that may remain. If necessary, the grinding process is repeated until a suitable fine powder results.

After the grinding process, the materials are blended to form a thick film paste. The functional materials are first measured out into the desired proportions, a percentage portion of solvent is then added and the mixture is blended at low speed until totally dissolved. At this point the binder is added, if desired the binder may be mixed with a suitable surfactant. The viscosity and the particle size of the blended paste is very important as it directly affects the thickness of the print and the line definition of the printed layers [15].

2.2 The screen printing process

The basic screen-printing process involves forcing a viscous paste through apertures of a stencil screen in order to deposit a pattern onto a substrate, as shown in Fig.1.

The final print dimensions and the level of registration achieved by this technique depend on various parameters. These parameters include: (i) emulsion thickness –see below (ii) screen gap, (iii) print pressure, (iv) squeegee hardness and (v) print speed.

Three sections comprise the screen: (i) the stencil (which defines the pattern to be printed), (ii) the mesh (which supports the stencil) and (iii) the frame (which supports the mesh). There is a choice between the use of screens or metal masks. While screens are relatively inexpensive, offer ease of use and can be imaged in-house, they tend to wear more quickly and offer less definition when compared to metal masks. Masks also offer the possibility of step-etching; this allows two different deposition thickness from the same mask. In summary, screens are more suitable for prototype work and short runs, while masks are used mainly for more substantial work and fine line work [19].

3. THE GAS SENSING MECHANISM

The gas sensing mechanism is based on changes in the resistance of the sensing material. There exists two main gas-sensing classes of semiconducting oxides. The first is in the detection of oxygen (e.g. for the monitoring of exhaust gases from internal combustion engines – also known as lambda sensors). These classes of sensor rely on bulk conductance changes induced by changes in oxygen partial pressure [20]. Semiconducting oxides that have been used as lambda sensors to respond to variations in oxygen partial pressure at elevated temperatures (700°C and above) [21]. These devices work by exploiting the balance between the bulk stoichiometry and the atmosphere. The change in electrical conductivity can be represented by equation (1)

$$\sigma = \sigma_0 \exp\left(-E_A / kT\right) p\left(O_2\right)^{1/n} \quad (1)$$

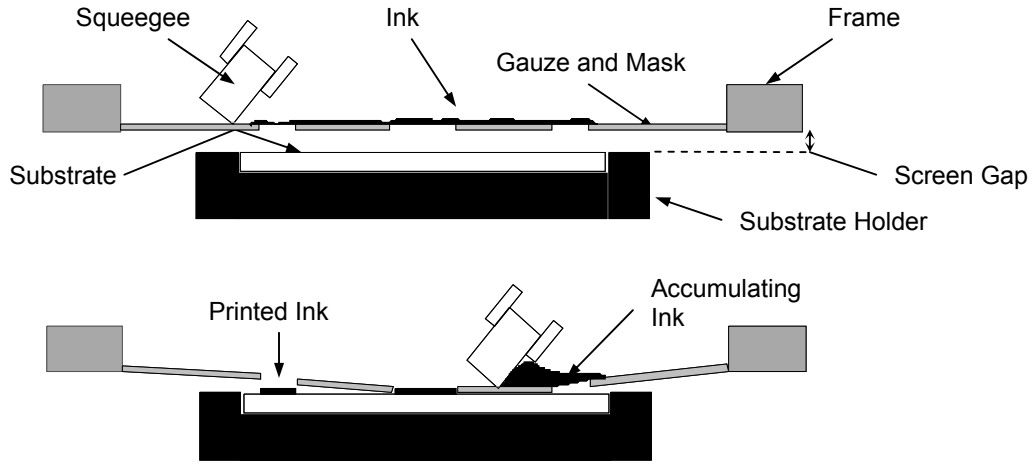

Fig. 1 Shows schematic arrangement of screen-printing system

where k is Boltzmann's constant, T is temperature in degrees Kelvin, E_A is the activation energy for conduction, $P(O_2)$ is the oxygen partial pressure and N is a constant determined by the dominant type of bulk defect [20].

The second major category in which semiconducting oxides find application is in an environment of fixed oxygen partial pressure (air), where they are used to detect the presence of minority gases. This is the response mechanism that applies to the sensors investigated in this study.

3.1 Minority gases in air response mechanism

Materials used to sense concentrations of reactive gases in air rely on changes in surface conductance. These changes in surface conductivity result from a displacement from equilibrium conditions caused by the presence of a gas [20]. The primary reaction controlling the gas response of the majority of semiconducting oxides operating in air ambient, involves the modulation of a universal surface species – the most likely candidate being surface oxygen ions (O_2^-) [22].These materials also prove sensitive to changes in oxygen partial pressure, however, since this remains effectively constant for this application, conductivity changes due to this phenomenon can be ignored [20]. In the formation of these oxygen ions at the gas/sensor interface, electrons are removed from the bulk – see Fig. 2.

In an n-type semiconductor for example, electrons are drawn via the conduction band from ionised donors, hence, the majority charge carrier density at the interface is reduced. This decrease in the majority charge carrier density results in the development of a potential barrier.

At the inter-grain boundaries a depletion layer is formed. It is this depletion layer at the junctions between the grains of the solid that comes to dominate the resistance of the material [20]. A sensing layer, if present in a porous form, can still exhibit large changes in resistance even if surface reactions modify the conductance only to a depth of the order of one micron or so [21]. Thus, semiconducting oxides can function as resistive gas sensors to monitor in air, any minority gases that can react in such a way as to modify the quantity of charge residing at the surface of the sensing layer. In the presence of a reactive gas such as carbon monoxide for example, the coverage of surface oxygen ions may be decreased and a fall in resistance is observed, due to the reduction in both the surface potential and the depletion length – see equation (2).

$$CO + O_2^- \rightarrow CO_2 + 2e^- \qquad (2)$$

For a p-type oxide semiconductor, the abstracted electrons from the bulk, has the effect of increasing the majority carrier (hole) concentration. Hence, a reaction with a gas

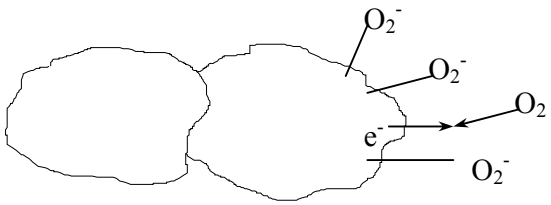

Fig. 2 The formation of oxygen ions at the grains of the oxide semiconductor surface, due to the abstraction of electrons from the bulk.

such as that shown in (2), would have the effect of freeing electrons, thus reducing the hole concentration and as a consequence the resistance rises [21].

The conductivity of some semiconducting oxides is also found to be affected by the presence of oxidising gases, nitrogen dioxide or chlorine for example. These gases are highly unlikely to react with surface oxygen ions, but are possibly reacting directly upon chemisorption, as described in equations (3) and (4).

$$NO_2 + e^- \leftrightarrow NO_2^- \quad (3)$$

and

$$Cl_2 + 2e^- \leftrightarrow 2Cl^- \quad (4)$$

From these reactions it can be seen that they serve to trap yet more electrons from the bulk. Hence, it is observed that responses take place in the opposite sense as compared to those with reducing gases [21]. Table 1 summarises the effect of oxidising and reducing gases on oxide sensing layers.

Another mechanism, in which oxide conductivity may be altered as a result of gas interaction, is via the creation of

Table 1. Summary of the effect of oxidising and reducing gases on n-type and p-type semiconducting oxides.

Material	Reducing gases	Oxidising gases
n-type	Resistance falls	Resistance rises
p-type	Resistance rises	Resistance falls

water molecules. Some oxide semiconductors have been found to be dependent on the ambient moisture content. Hence, when a surface catalysed reaction leads to the formation of water, e.g.

$$H_2 + O^{2-} \leftrightarrow H_2O + 2e^- \quad (5)$$

the water itself may have an effect on the conductivity response, in addition to the release of electrons. However, in general, resistance changes due to moisture changes in the atmosphere are undesirable in relation to gas sensing [21].

In certain cases it has been reported that number of n-type materials have been found to exhibit p-type characteristics [23]. Conductivity sometime changes from a p-type to n-type, and vice-versa. For example TiO_2 at low oxygen partial pressures the n-type semiconductor but with increase oxygen partial pressures (above some minimum conductance values) switches from n-type to p-type. Some oxide semiconductors such as $BiFe_4Nb_6O_{30}$ have been known to exhibit resistance decreases to both oxidizing and reducing gases at concentrations of 1% in air. The oxide semiconductor possibly switches from n-type to p-type or vice versa. Under normal conditions $BaSn_{0.9}Zr_{0.1}O_3$ has shown a p-type to n-type transition with increasing hydrogen concentration [23].

4. METHODS FOR REPRESENTING SENSOR RESPONSE

Methods for presenting the response of a sensor vary from one paper to another. Here some examples, which have been used by different authors to represent the response of a gas sensitive device, are presented. In the case of a chemical sensor based on changes in resistance or conductance with respect to variations in the input concentration of a gas, Table 2 presents some of the more common parameters, which have been used to represent sensor response. In this paper the percentage relative resistance change was the parameter chosen to represent sensor response, with the slope of the response curve representing sensor sensitivity.

5. EXPERIMENTAL

In this study three ratios of iron oxide to zinc oxide were used to form thick film pastes. The first ratio (sample 1) was 90% mol Fe_2O_3/10%mol ZnO, the second ratio (sample 2) was, 80% mol Fe_2O_3/20% mol ZnO and the third ratio (sample 3) was 70% mol Fe_2O_3/30% mol ZnO. Each sample was mixed and wet-ball milled in alcohol for 24h to ensure that both powders formed a homogenous mixture. The mixture was dried at 120˚C to evaporate the alcohol. 20 grams from each sample was then pressed at 2 tons of pressure to make pellets using die. To change the properties of the materials, all pellets were isostatically pressed and fired at 1250˚C at a rate of 5˚C/min, under a vacuum of $6x10^{-3}$ mbar for 5h, followed by cooling at a rate of 3˚C/min. The pellets were then broken up and ground down to a powder using a Gy-RO Mill machine for 7mintues.

Polyvinyl butyral (7wt%) was used as a binder, while ethylenglycolmonobutylether served as a solvent to make a suitable paste. Silver electrodes were printed onto glass substrates; an interdigitated pattern was used to improve the admittance of the

Table 2. Common parameters used to represent sensor response.

Name	Parameter		Used by
Relative resistance	$\frac{R_{gas}}{R_{air}}$	$\frac{R_{air}}{R_{gas}}$	Tianshu et al. [26]
Relative resistance change	$\frac{(R_{gas}-R_{air})}{R_{air}}$	$\frac{(R_{air}-R_{gas})}{R_{air}}$	Bhooloka Roa [10]
Percentage relative resistance change	$\frac{(R_{gas}-R_{air})}{R_{air}}x100$	$\frac{(R_{air}-R_{gas})}{R_{air}}x100$	Srivastava et al. [25]
Relative conductance	$\frac{G_{gas}}{G_{air}}$	$\frac{G_{air}}{G_{gas}}$	Carotta et al. [8]
Relative conductance change	$\frac{(G_{gas}-G_{air})}{G_{air}}$	$\frac{(G_{air}-G_{gas})}{G_{air}}$	Patel et al. [13]
Percentage relative conductance change	$\frac{(G_{gas}-G_{air})}{G_{air}}x100$	$\frac{(G_{air}-G_{gas})}{G_{air}}x100$	More et al. [27]

material. The paste was then screen-printed on top of these electrodes. Fig. 3 shows the sensor electrode configuration. Different designs of electrodes have been used in gas sensors, but the interdigitated silver electrode structure has become the most common [2, 24, 25].

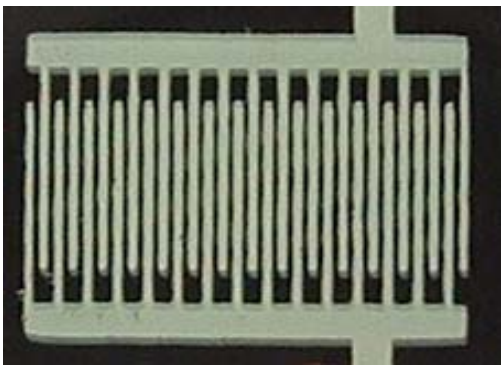

Fig. 3 Sensor electrode configuration. The gap between electrodes is 0.2mm.

5.1 Testing apparatus and procedure

For the experimental tests, the sensors were placed in a gas chamber of volume 2000cc. Fig. 4 shows a diagram of the test chamber used. The volume of liquid needed to give a specific vapor concentration (C_{ppm}) was calculated using equation (6):

$$V = \frac{C_{ppm}.V_a.M}{24.5\times10^9.D} \quad (6)$$

where V is the required liquid volume, V_a is the volume of the dilutant air (equal to the volume of the test chamber) and M is the molecular weight of the liquid.

The sensors were used to detect methanol, ethanol and propanol vapors at room temperature in the concentration range 500 - 2000ppm.The readings were taken 10 minutes after gas setting had occurred. The percentage relative

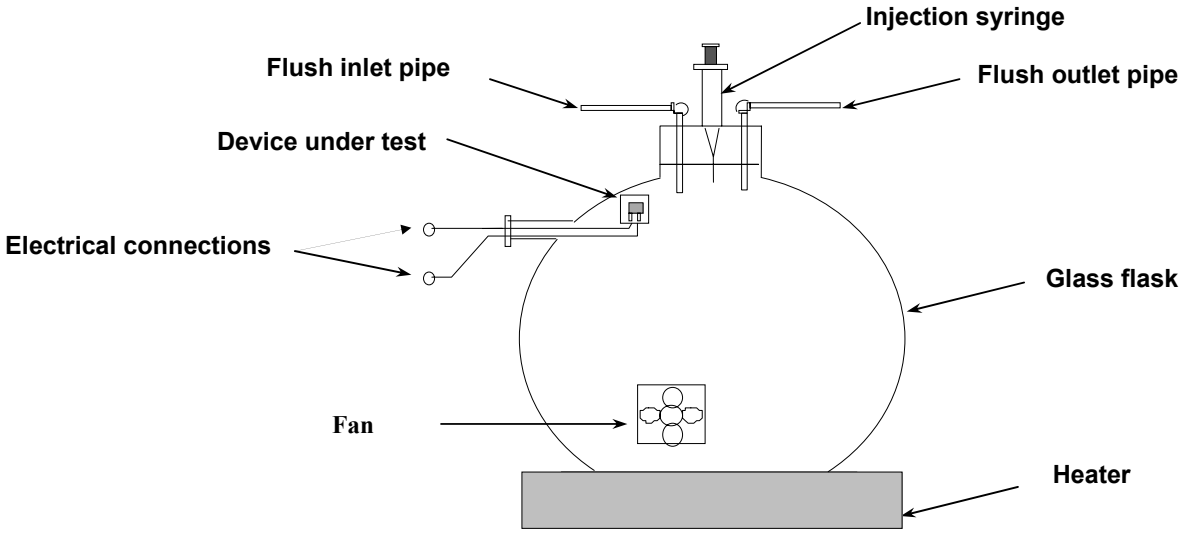

Fig. 4 Schematic diagram of the test chamber used to measure the alcohol vapour responses.

resistance change (ΔR) is defined in equation (7):

$$\Delta R = \left(\frac{R_{gas} - R_{air}}{R_{air}} \right) \times 100 \quad (7)$$

where R_{gas} is the resistance of the sensor after exposure to a gas and R_{air} is the resistance of the sensor in air (baseline resistance).

6. RESULT AND DISCUSSION

6.1 Material properties

6.1.1 X-ray diffraction analysis

It is well known that variance in different parameters such as the milling speed; applied pressure in the creation of pellets and the firing temperature during fabrication leads to changes in the structures and compositions of the sensing layers. X-ray diffraction analysis (XRD) is employed to determine the final composition of the materials [28]. XRD is also used to calculate the crystallites size according to the Scherer equation [29].

In this study XRD analysis (from 10˚ to 70˚, 2θ) was used to examine the final compositions of the samples. Fig. 5 shows an XRD of sample 1, from this data it can be seen that the main phase in the final composition of this sample is zinc ferrite ($ZnFe_2O_4$) and α- iron oxide (α-Fe_2O_3). This can be explained by the chemical reaction of Fe_2O_3 with ZnO at 1250˚C – see equation (8).

$$Fe_2O_3 + ZnO \rightarrow ZnFe_2O_4 + \alpha\text{-}Fe_2O_3 \quad (8)$$

Fig. 6 shows the results of the X-ray diffraction analysis for sample 2. This data shows that the final composition of this sample consists of, only one phase, this being zinc ferrite ($ZnFe_2O_4$). No peaks were observed for α- Fe_2O_3 and ZnO, this means that the zinc oxide and iron oxide were completely consumed to form the $ZnFe_2O_4$ phase – see equation (9).

$$Fe_2O_3 + ZnO \rightarrow ZnFe_2O_4 \quad (9)$$

Fig. 7 shows the results of the X-ray diffraction analysis for sample 3.This data shows that the final composition of this sample consists of, $ZnFe_2O_4$ and ZnO. This reaction is explained by the following equation:

$$Fe_2O_3 + ZnO \rightarrow ZnFe_2O_4 + ZnO \quad (10)$$

From equations 8, 9 and 10 and according to the X-ray diffraction results, it can be concluded that:

(i) Three small peaks were exhibited due to the presence of α- Fe_2O_3 in sample 1.
(ii) Only zinc ferrite was formed as no peaks were observed for α- Fe_2O_3 and ZnO for sample 2.
(iii) Three small peaks of ZnO were observed in sample 3.

From the above results it is noted that the final compositions of samples 1, 2 and 3 are quite similar, also if the small peaks in the XRD results are ignored, it can be said that the main composition of the three samples is zinc ferrite ($ZnFe_2O_4$).

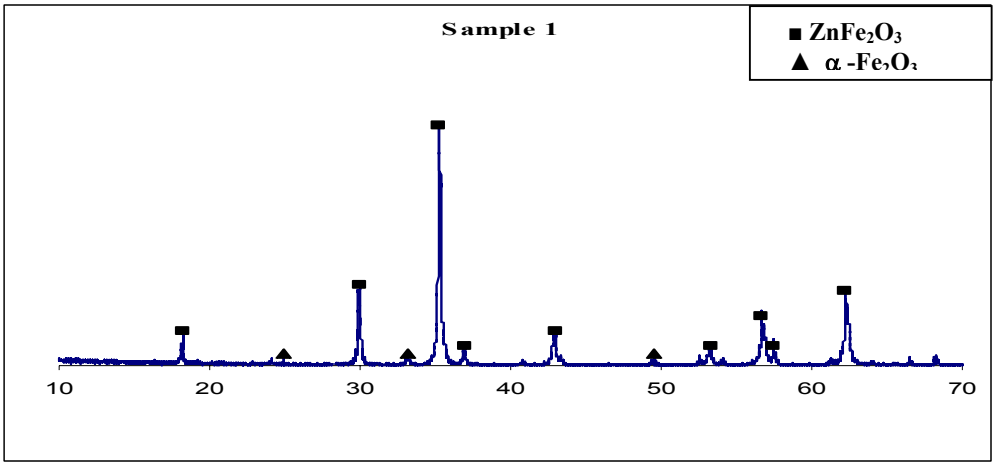

Fig. 5 X-ray diffraction analysis for sample 1.

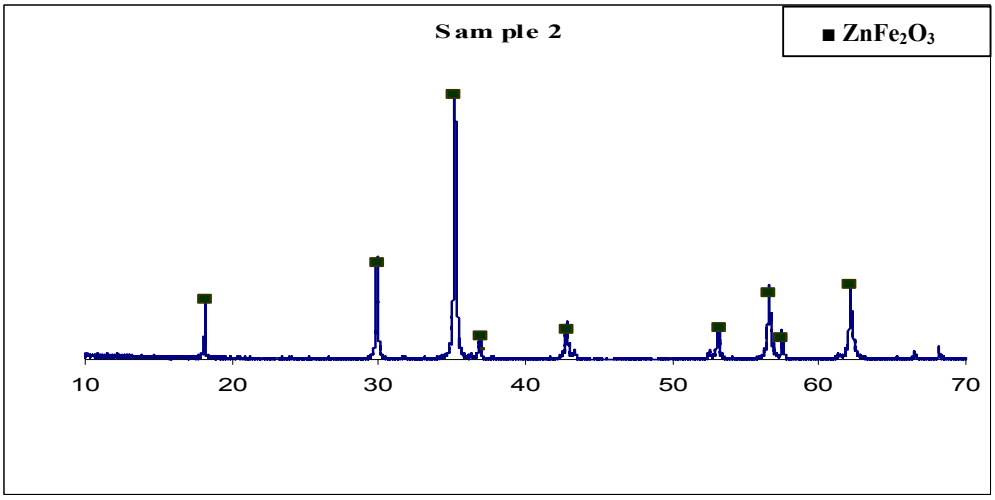

Fig. 6 X-ray diffraction analysis for sample 2.

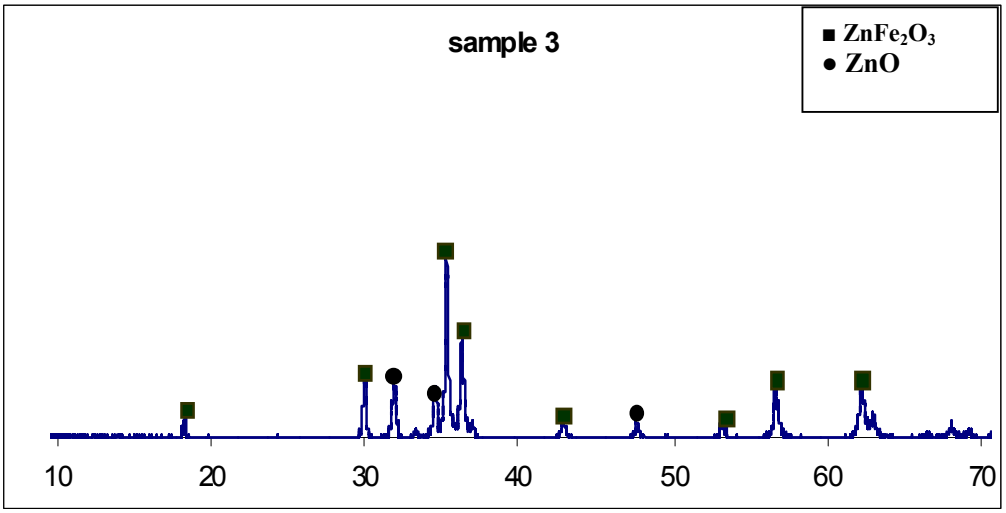

Fig. 7 X-ray diffraction analysis for sample 3.

6.1.2 Scanning electron microscopy

Scanning electron microscopy (SEM) is used to study the microstructure of the materials and often is used in thin and thick film studies to calculate the grain size of the powders. Many studies have used this technique such as Xu *et al.[3]*, Qu *et al* [30]., Wang *et al.* [31] and Pignataro *et al*. [32].

In this paper scanning electron microscopy was used to calculate the grain size of the powders and to view the surfaces of the printed films.

Figs. 8 and 9 show the scanning electron microscopy photos of the film surface and the powder of sample 1 respectively. From these SEM images, it can be noted that the average grain size of the powder is about 12μm.

Figs. 10 and 11 show SEM pictures of the film surface and the powder for sample 2 respectively, with the average grain size of the sensing powder estimated to be about 8 - 10μm. Figures 12 and 13 show SEM images of the sensing layer surface and the powder for sample 3 respectively. The SEM showed that sample 3 had a smallest grain size (~5μm) of all the samples analysed. From the above SEM figures it can be seen that there are differences in grain size between samples 1, 2 and 3, with sample 3 showing the smallest grain size. It was observed that the addition of Zn increases the sensitivity by decreasing the grain size of the materials. This is in agreement with the findings of Neri *et al*. [5], where Fe_2O_3 and ZnO was used to detect NO_2.

In this study it was seen that the grain size of the materials decreased from 12 to 8 to 5μm for sample 1, 2 and 3 respectively although they were fabricated under the same conditions. This change may be attributed to an increase in the zinc-oxide and a decrease in the iron-oxide.

The decrease in grain size also lowers the working temperature of the devices due to an increase in the surface area [3]. It has been reported also that the grain size of some materials can be affected by firing and/or annealing temperatures, for example, Steffes *et al.* used In_2O_3 in the form of thin films to detect NO_2, the grain size was seen to increase from 20 to 40nm after annealing at a temperature of 800°C [33]. Kim *et al*. [34] used In_2O_3/Fe_2O_3 as a thick film gas sensor to detect ozone, SEM images of these materials did not show any difference in the sensing layers after firing at 900˚C, but the grain size was seen to grow substantially after firing at a temperature of 1300°C. It has been reported that pure titania films fired at 650°C showed grain size at the nanometric level, however firing at 850°C induced a substantial grain growth of more than one order of magnitude, up to 400nm [29]. In a study by Guidi *et al.* [18], it was seen that firing of TiO_2 at a temperature of 1100°C resulted in a much broader average grain size distribution.

6.2 Sensor responses to alcohol vapors

The relative resistance change of the sensors was found to increase linearly with increasing the gases vapor concentration for the three sensors. The sensitivities for the three sensors were calculated from the slope of the graphs. Fig. 14 shows the percentage relative resistance change for sensor 1 ($ZnFe_2O_4/\alpha\text{-}Fe_2O_3$) with increasing gas concentration. The percentage relative resistance change was seen to increase linearly with increasing gas concentration at room temperature. The sensor exhibited the highest response to propanol (with the sensitivity calculated to be 0.077%/ppm), the second highest response to ethanol (with the sensitivity calculated to be 0.024%/ppm) and the lowest response to methanol (with the sensitivity calculated as 0.01%/ppm).

Fig. 15 shows the sensitivity of sensor 1 ($ZnFe_2O_4/\alpha\text{-}Fe_2O_3$) to methanol, ethanol and propanol at room temperature.

Fig. 16 shows the percentage relative resistance change of the sensor 2 ($ZnFe_2O_4$) with increasing gas concentration. The sensor exhibited the highest response to propanol (0.166%/ppm) in comparison to that of ethanol (0.037%/ppm) and methanol (0.007%/ppm).

Fig. 17 shows the sensitivity of the sensor 2 ($ZnFe_2O_4$) for methanol, ethanol and propanol at room temperature.

Fig. 18 shows the percentage relative resistance change of sensor 3 ($ZnFe_2O_4$/ZnO) with increasing gas concentration. The sensitivity of the sensor to methanol, ethanol and propanol was: 0.006%/ppm,.015%/ppm and 0.173%/ppm respectively.

Fig. 19 shows the sensitivity of the sensor 3 ($ZnFe_2O_4$/ZnO) to methanol, ethanol and propanol at room temperature.

From the above results, it is observed that:

(i) The three sensors display more or less the same sensitivity to methanol vapors.
(ii) It was found that the sensitivity of sensor 1 and 2 to ethanol increased from 0.024 to 0.037%/ppm but decreased to 0.015%/ppm for sensor 3.
(iii) The three sensors exhibited excellent sensitivity to propanol, from 0.077%/ppm to 0.166%/ppm to 0.173%/ppm for sensor 1, sensor 2 and 3 respectively
(iv) All three sensors exhibited a higher sensitivity to propanol, followed by the next highest sensitivity to ethanol and lowest sensitivity to propanol. These differences in sensitivities are due to the effects of one or more factors, which will subsequently be discussed.

As Figs. 17, 19 and 15 show, all sensors exhibit a much higher sensitivity to propanol, in

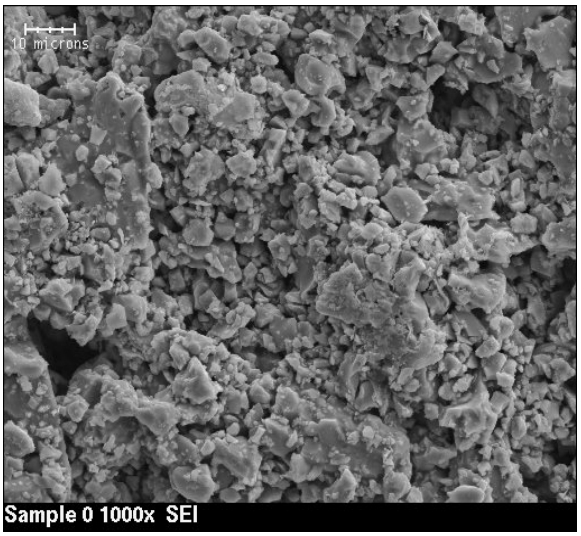

Fig. 8 Scanning electron microscopy of film surface on the glass substrate for sample 1, 90% mol Fe_2O_3/10% mol ZnO.

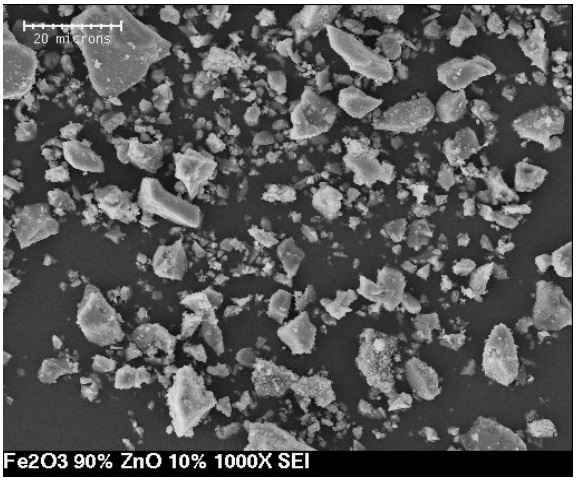

Fig. 9 Scanning electron microscopy of the prepared powders on the glass substrate for sample 1, 90% mol Fe_2O_3/10% mol ZnO.

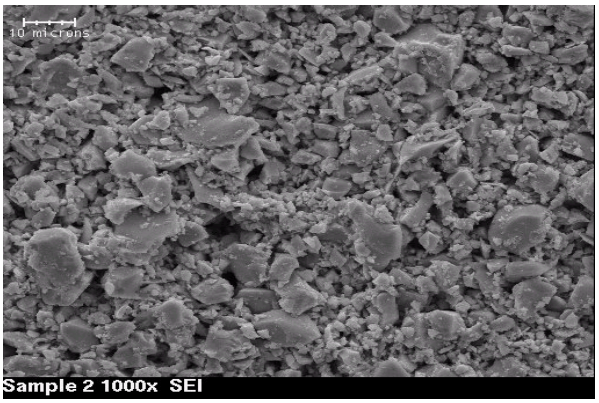

Fig. 10 Scanning electron microscopy of film surface on the glass substrate for sample 2, 80% mol Fe_2O_3/20 %mol ZnO.

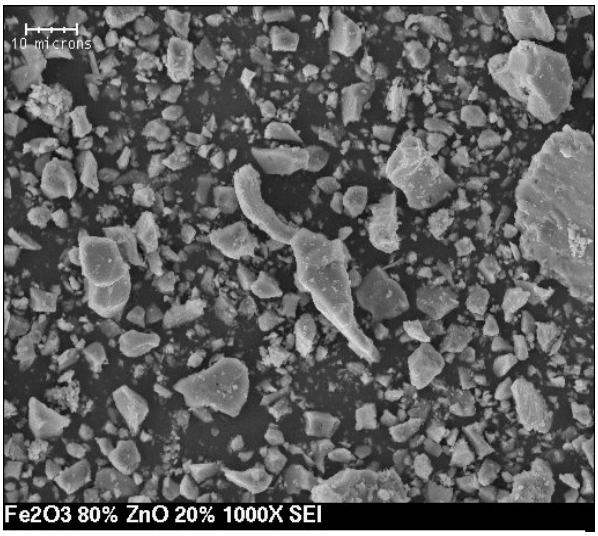

Fig. 11 Scanning electron microscopy of prepared powders on the glass substrate for sample 2, 80% mol Fe_2O_3/20% mol ZnO.

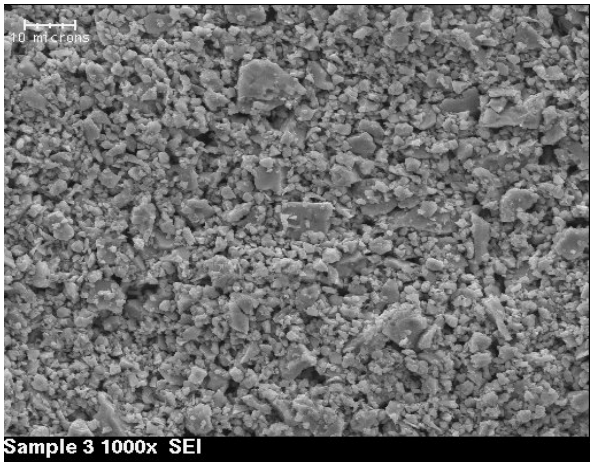

Fig. 12 Scanning electron microscopy of film surface on the glass substrate for sample 1, 70% mol Fe_2O_3/30% mol ZnO.

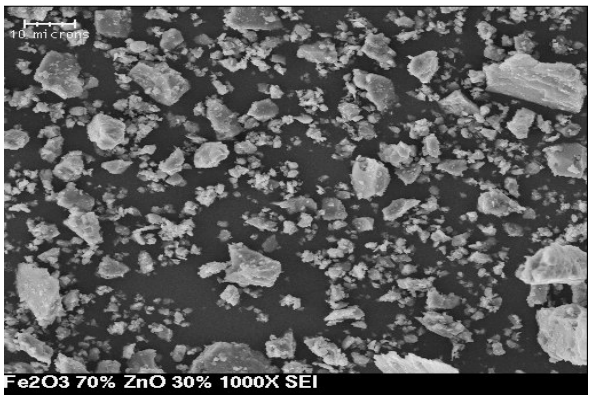

Fig. 13 Scanning electron microscopy of prepared powders on the glass substrate for sample 1, 70% mol Fe_2O_3/30% mol ZnO.

comparison to their sensitivity to methanol and ethanol. Moreover, it was observed that the composition ratio of Fe_2O_3 to ZnO influenced the sensitivity of the sensor towards propanol vapor. Propanol sensitivity was seen to increase from 0.077 to 0.166 to 0.173%/ppm for the sensors with molecular weight composition ratios 90%/10%, 80%/20%, and 70%/30% of Fe_2O_3 to ZnO respectively.

The gas sensing mechanism is based on changes in the

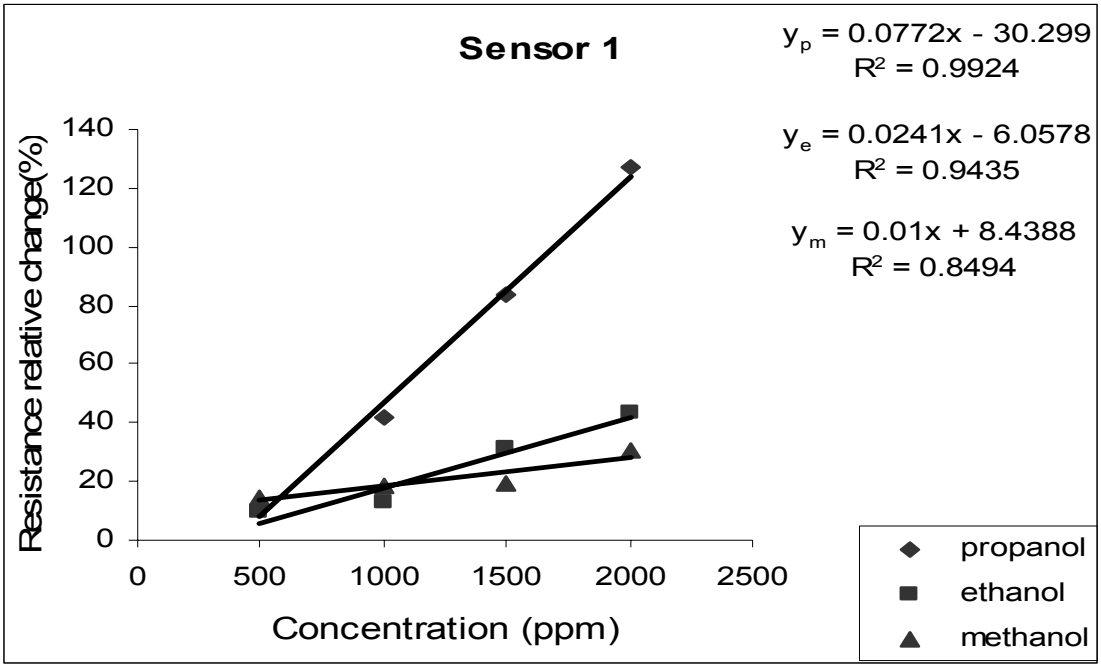

Fig. 14 The percentage relative change in resistance with increasing gas vapour concentration for sensor 1.

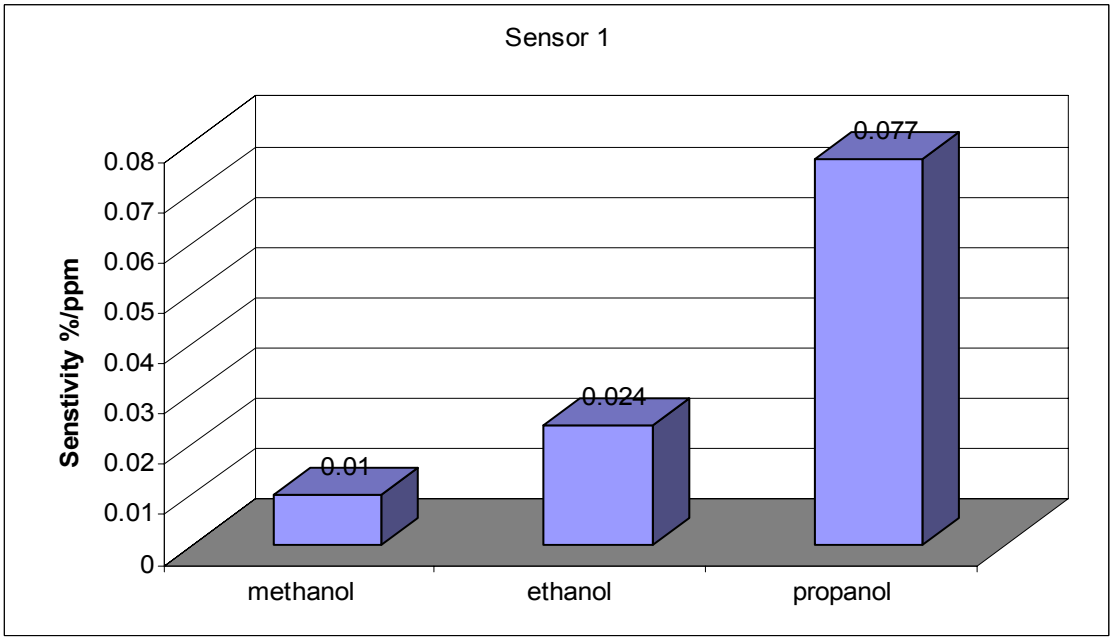

Fig. 15 The sensitivity of the sensor 1 to methanol, ethanol and propanol.

resistance of the sensing material. This resistance change depends on the following parameters (some of which have been discussed previously in section 3):

The particle size: It is well known that gas sensitivity is correlated to grain size, oxygen adsorption quantity and the active energy of oxygen adsorption.

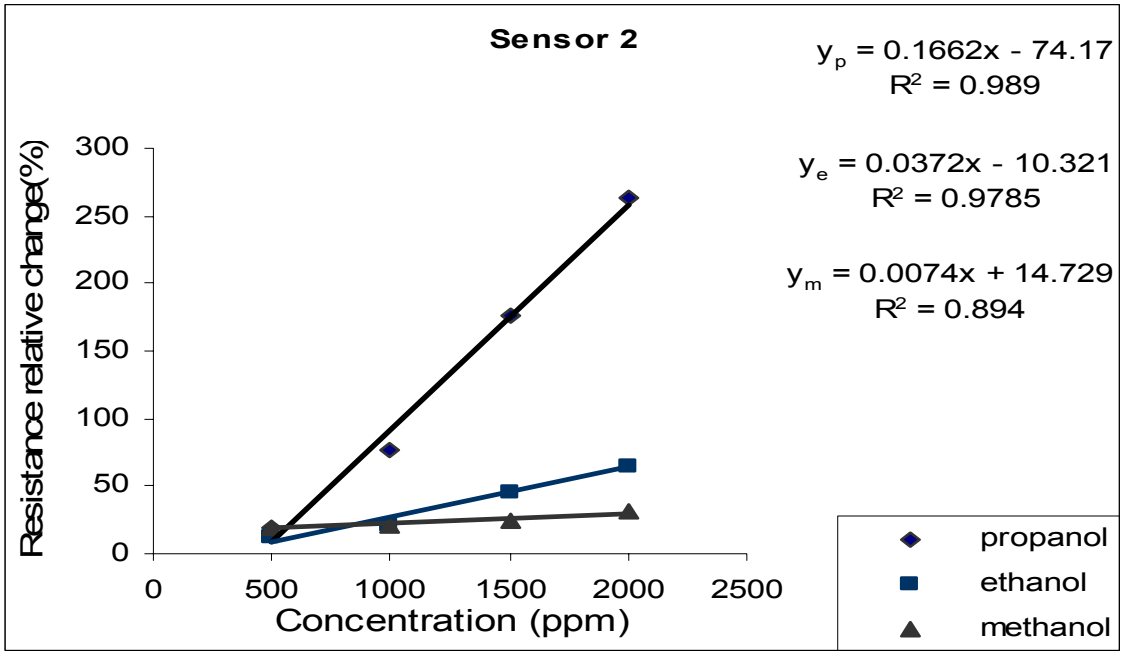

Fig. 16 The percentage relative change in resistance with increasing gas vapour concentration for sensor 2.

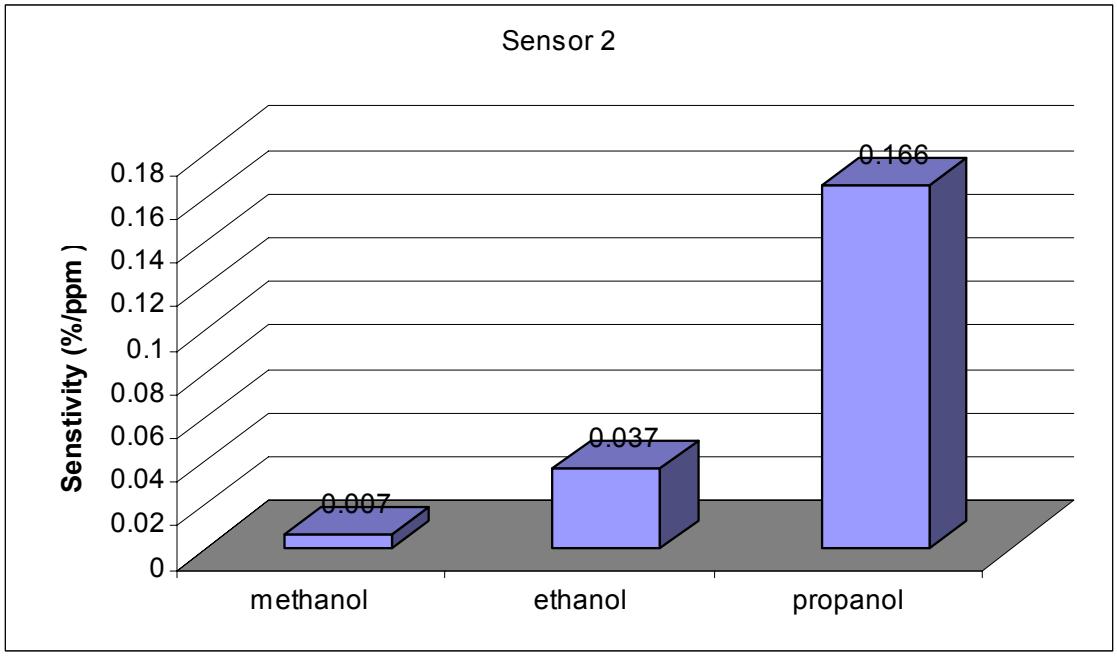

Fig. 17 The sensitivity of the sensor 2 to methanol, ethanol and propanol.

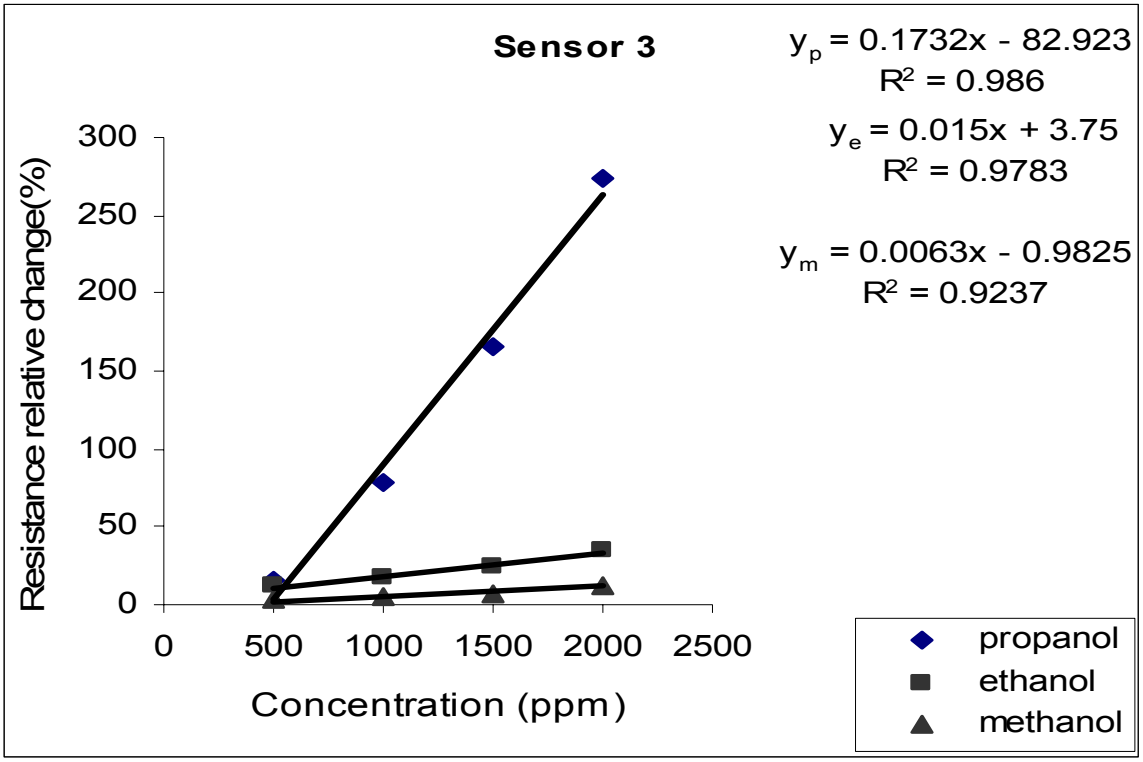

Fig. 18 The percentage relative change in resistance with increasing gas vapour concentration for sensor 3.

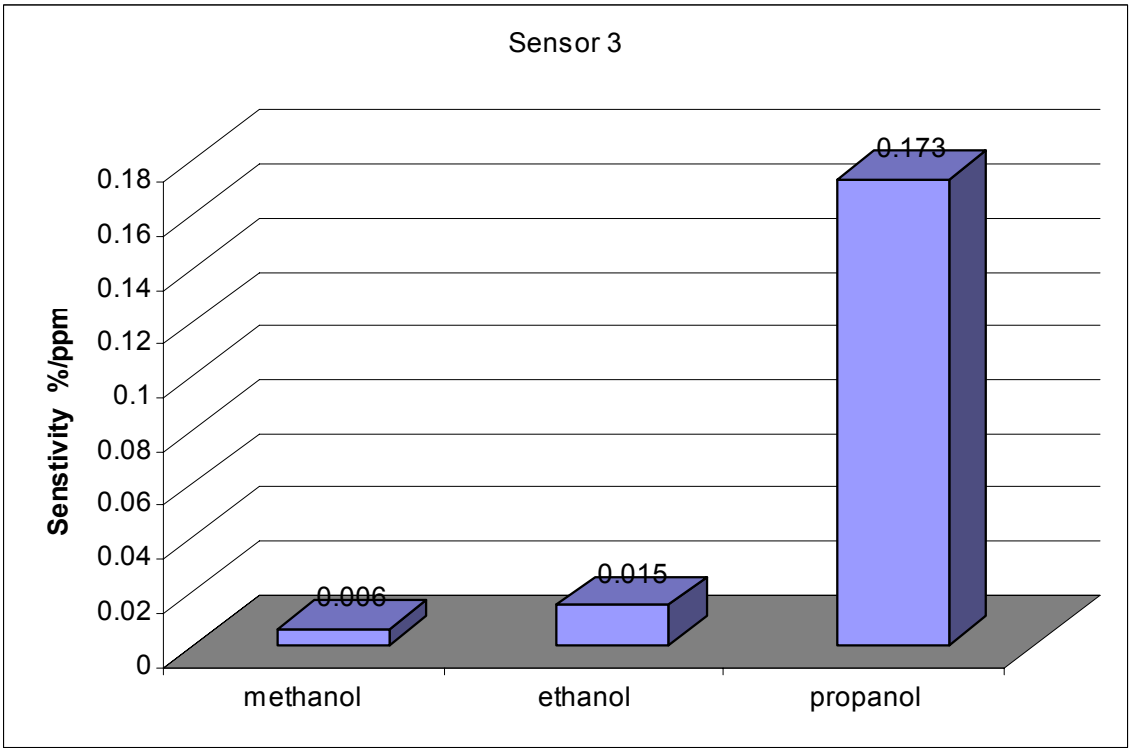

Fig. 19 The sensitivity of the sensor 3 to methanol, ethanol and propanol.

The smaller the grain size, the larger the specific surface area, which results in greater oxygen adsorption and higher sensitivity, and vice versa [3]. The average grain size of sensors 1, 2 and 3 were 12, 10 and 5μm respectively. As consequence, sensor 3 proved to have the highest sensitivity to propanol, due to it having the smallest grain size. Sensor 2 had the second the smallest grain size; hence, it had the second highest sensitivity to propanol. Sensor 1 had the highest grain size and as expected it displayed the lowest sensitivity.

Type of the sensing materials: the electrical conductivity of p-type semiconductors increases reducing gases are adsorbed on their surface. The opposite occurs for n-type semiconductors – see Table 1. The sensors fabricated in this study displayed p-type behaviour. Electrons are captured from the sensing layers, which results in an increase in the hole concentration. The reducing gases acting on the $ZnFe_2O_4$ sensor surfaces can be explained by equation (11)

$$R + O^-_{(ads)} \leftrightarrow RO + e^- \quad (11)$$

where R is the reducing gas, O^- is the oxygen ion adsorption and e^- are electrons. This reaction shows an increase in the number of electrons (this reaction infuses electrons into $ZnFe_2O_4$ sensing material) [6]. This leads to a decrease in holes concentration (majority carriers in p-type semiconductors) resulting in a decrease in the value of the current (I) through the sensor. This is observed as an increase in resistance, the magnitude of this observed change being proportional to the concentration of the reducing gas.

Type of acceptor and donor: When a reactive gas is adsorbed on the surface, the carrier density is altered; this results in a conductivity change. This change depends on the chemical characteristics of the acceptor and donor centres [4, 35]. The different chemical characteristics of the acceptors and donors for the three sensors under test, results in differing amounts of adsorbed gases on their respective sensing surfaces. As a consequence the three sensors display different sensitivities to propanol, methanol and ethanol vapors.

6.3 Response and recovery time

The response time of a sensor can vary from seconds to minutes, but short response and recovery times are desirable sensor characteristics. In the testing of these sensors, the response time was defined as the time taken to achieve 90% of the final change in the resistance, following a 0-1000ppm step change in vapor concentration. The response times for the three sensors were calculated as 48.6s, 86.4s and 76.5s respectively. At a given time (after the steady-state response) the alcohol vapor was flushed from the system to determine the recovery times for the three sensors. The respective recovery times for the three sensors were calculated as 117s, 189s and 153s. Fig. 20 shows the graphs from which the response and recovery times were calculated.

Sensor 1 shows the fastest response and recovery times while sensor 2 shows slowest response and recovery times. It was found that the recovery times were longer than the response times for the three sensors. It is well known that the response time is a function of gas adsorption and recovery time is a function of gas desorption. Adsorption is an exothermic process, whereas desorption requires external energy for the molecules (gas or water) to depart from the sensors surface [30], for this reason the recovery times were longer than the response times.

7. CONCLUSION

In this paper the gas sensing properties of zinc ferrite (p-type semiconductor) polymer thick films were investigated. It was observed that:

(i) The propanol sensitivity increased from 0.077 to 0.166 to 0.173%/ppm for the sensors with composition ratios 90/10%Mwt, 80/20%Mwt, and 70/30%Mwt of Fe_2O_3 to ZnO respectively.

(ii) An increase in the amount of ZnO results in a decrease in the grain size of the sensing material, and hence, there is an increase in the sensitivity to propanol at room temperature.

(iii) The response times of the three sensors to a 0 to 1000ppm step change to propanol vapor concentration were 48.6s, 86.4s and 76.5s for three samples respectively.

(iv) The recovery times of three sensors to propanol following removal of the 1000ppm vapor concentration were 117s, 186s and 153s respectively.

(v) The three sensors proved to be more sensitive to propanol vapor than to methanol and ethanol vapor.

From the above if is clear that Fe_2O_3/ZnO thick-films can function effectively as sensitive and selective gas sensors. Due largely to their ability to operate at room temperature (hence, low power consumption) and low fabrication costs (afforded by screen-printing), these sensor devices fulfil the requirements for many industrial applications, especially portable, sensor array based measurement instruments, such as the electronic nose.

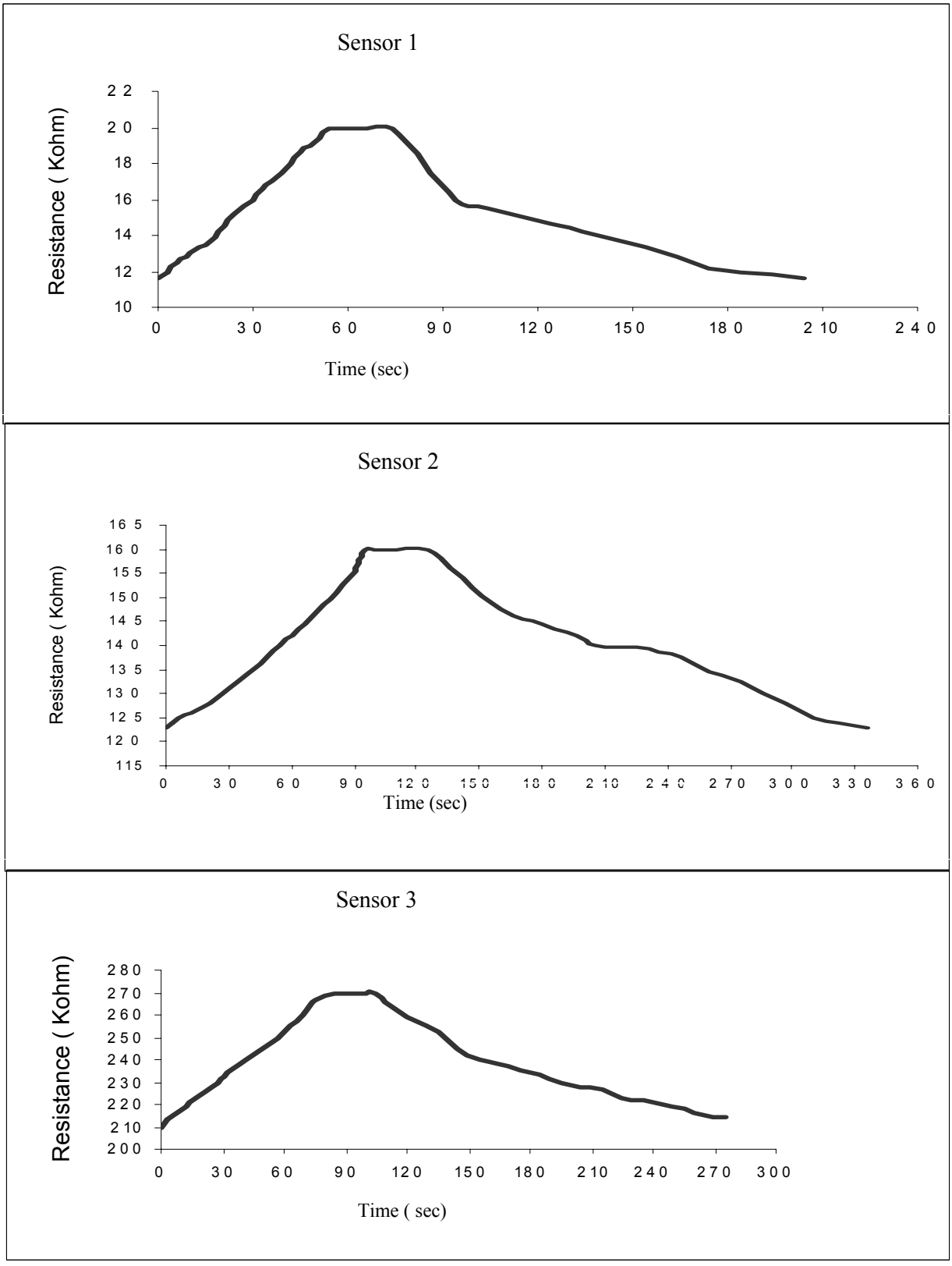

Fig. 20 Response and recovery characteristics of sensors 1, 2 and 3 following 1000ppm step changes in propanol vapour concentration at room temperature

References

[1] S. Harbeck, A. Szatvanyi, N. Barsan, U.Weimar, V. Hoffmann "DRIFT studies of thick film un-doped and Pd-doped SnO2 sensors: temperature changes effect and CO detection mechanism in the presence of water vapour" Thin Solid Films, Vol **436**. pp. 76-83, 2003.

[2] A .Ahmad,., J. Walsh, and T.A. Wheat "Effect of processing on the properties of tin oxide-based thick-film gas sensors" Sensors and Actuators B: Chemical, Vol.**93**(1-3): pp, 538-545,2003..

[3] J.Xu, Q. Pan, Y Shun,Z. Tian " Grain size control and gas sensing properties of ZnO gas sensor" Sensors and Actuators B: Chemical,.Vol.**66**(1-3): pp. 277-279,2000.

[4] M.R. Islam,., N. Kumazawa, and M. Takeuchi, "Titaniumdioxide chemical sensor working with AC voltage". Sensors and Actuators B: Chemical, Vol.46, pp, 114-119,1998.

[5] G. Neri,A . Bonavita , S. Galvagno , P. Siciliano , S Capone " CO and NO2 sensing properties of doped-Fe2O3 thin films prepared by LPD ". Sensors and Actuators B: Chemical, Vol. **82**(1),pp, 40-47,2002.

[6] Y.Wang, J. Chen, and X. Wu " *Preparation and gas-sensing properties of perovskite-type SrFeO3 oxide "* Materials Letters,.Vol **49**, pp, 361-364,2001.

[7] C.Xiangfeng, L. Xingqin, and M. Guangyao, " Effects of CdO dopant on the gas sensitivity properties of ZnFe2O4 semiconductors ". Sensors and Actuators B: Chemical, Vol. **65**(1-3), pp. 64-67,2000.

[8] M.Carotta, G. Martinelli, Y. Sadaoka, P. Nunziante , E. Traversa "Gas-sensitive electrical properties of perovskite-type SmFeO3 thick films" Sensors and Actuators B: Chemical, Vol.**48**(1-3) pp, 270-276,1998

[9] G.Sberveglieri,E. Comini, G. Faglia, W. Wlodarski " Titanium dioxide thin films prepared for alcohol microsensor applications" Sensors and Actuators B: Chemical,. **66**(1-3) pp, 139-141, 2000.

[10] B. Rao, "Zinc oxide ceramic semi-conductor gas sensor for ethanol vapour" Materials Chemistry and Physics,Vol. **64**(1.pp, 62-65), 2000.

[11] G.Martinelli, M. Carotta , M. Ferroni, Y. Sadaoka E. Traversa " *Screen-printed perovskite-type thick films as gas sensors for environmental monitoring "* Sensors and Actuators B: Chemical, Vol. 55(2-3) pp,99-110,1999.

[12] E.Schaller, J. Bosset, and F. Escher, " Electronic Noses' and Their Application to Food ". Lebensmittel-Wissenschaft und-Technologie, Vol. 31(4), pp, 305-316,1998.

[13] N.G Patel, P.D. Patel, and V.S. Vaishnav, "Indium tim oxide (ITO) thin film gas sensor for detection of methanol at room temperature". Sensors and Actuators B: Chemical, Vol. **96** (1-2),pp 180-189,2003.

[14] M.Prudenziati, ed. "*Thick Film Sensors*. Handbook of Sensors and Actuators", ed. S. Middelhoek. Vol. 1. 1994, Elsevier: Amsterdam.

[15] C. Harper, ed. "Handbook of thick film hybrid microelectronics" 1974, McGraw-Hill.

[16] K.Arshak, K.Twomey and.D.Egan., " A ceramic thick film Humidity sensor Based on MnZn Ferrite. Sensors" Vol, **2**. pp, 50-61,2002.

[17] W. Noh, Y. Shin, J. Kim, W. Lee, K. Hong, Sheikh, A. Akbar and J.Park "Effects of NiO addition in WO3-based gas sensors prepared by thick film process" Solid State Ionics, **152-153**: p. 827-832,2002.

[18] V.Guidi, M. Butturi, M. Carotta, B. Cavicchi ,M. Ferroni, C. Malagu,G.Martinelli,D Vincenzi, M. Sacerdoti, M. Zen, " Gas sensing through thick film technology" Sensors and Actuators B: Chemical Vol. **84**(1) , pp, 72-77,2002.

[19] C.J Ryan "*The design and development of piezoelectric polymer/cermet thick fim SAW devices*, in *Department of Electronic and Computer Engineering*" 2000, University of Limerick: Limerick. pp, 153.

[20] P.T Mosoley,. and B.C. Tofield, eds. "Solid State Gas Sensors". 1987, Adam Hilger: Bristol.

[21] P.T., Mosoley "*Solid state gas sensors.* Measurement" Science and Technology, Vol. **8** , pp, 223-237,1997.

[22] P.T.Mosoley, J.O.W. Norris, and D.E. Williams, eds. "Techniques and Mechanisms in Gas Sensing" The Adam Hilger Series on Sensors. 1991, IOP Publishing: Bristol.

[23] P.T., moseley, *Thich film Semiconductor Gas Sensors.*Vol. **1,** pp. 289-360,1994.

[24] G. Reddy,W. Cao, O. Tan , W. Zhu , S. Akbar "Selective detection of ethanol vapor using xTiO2-(1 - x)WO3 based sensor" Sensors and Actuators B: Chemical,Vol. **94**(1) , pp, 99-102,2003.

[25] A.K., Srivastava "Detection of volatile organic compounds (VOCs) using SnO2 gas-sensor array and artificial neural network" Sensors and Actuators B: Chemical, **96**(1-2) pp, 24-37,2003.

[26] Z.. Tianshu, P. Hing , Y.Li, Z. Jiancheng "Selective detection of ethanol vapor and hydrogen using Cd-doped SnO2-based sensors". Sensors and Actuators B: Chemical,Vol. **60,** pp, 208-215,1999.

[27] P. More, Y. Khollam, S.Deshpande, S. Date,N. Sali, S. Bhoraskar, S. Sainkar, R. Karekar ,R. Aiyer. " *Introduction of Al2O3/Cu2O material of H2 gas sensing applications.* Materilals Letters,Vol. **58,** pp,1020-1025,2004.

[28] O.K Tan,W. Cao,W. Cao, W. Zhu,J. Chai, J. Pan "*Ethanol sensors based on nano-sized [alpha]-Fe2O3 with SnO2, ZrO2, TiO2 solid solutions"* Sensors and Actuators B: Chemical, Vol. **93** (1-3),pp, 396-401,2003.

[29] C. Cantalini,W.Wlodarski, H. Sun, M. Atashbar, M. Passacantando ,S. Santucci "NO2 response of In2O3 thin film gas sensors prepared by sol-gel and vacuum thermal evaporation techniques" Sensors and Actuators B: Chemical. Vol. **65**(1-3), pp, 101-104,2000.

[30] W.Qu and J.-U. Meyer,"A novel thick film ceramic humidity sensor". Sensors and Actuators B: Chemical, Vol. **40,** ,pp,175-182,1997.

[31] L.Wang and R.V. Kumar "Thick film miniaturized HCl gas sensor". Sensors and Actuators B: Chemical, Vol.**98**, ,pp, 196-203,2004.

[32] B. Pignataro, S. Conoci, L. Valli, R. Rella ,G. Marletta "Structural study of meso-octaethylcalix[4]pyrrole Langmuir-Blodgett films used as gas sensors" Materials Science and Engineering C. Vol.19, pp, 27-31,2002.

[33] H.Steffes,C.Imawan,F.Solzbacher,E. Obermeier "Enhancement of NO2 sensing properties of In2O3-based thin films using an Au or Ti surface modification". Sensors and Actuators B: Chemical,Vol. **78**(1-3), pp, 106-112,2001.

[34] S.-R. Kim, H-K Hong, C-H Kwon, D-H Yun,K. Lee, Y-K Sung "Ozone sensing properties of In2O3-based semiconductor thick films". Sensors and Actuators B: Chemical, Vol. **66**(1-3), pp, 59-62,2000.

[35] M.Islam, N. Kumazawa, and M. Takeuchi, "Chemical sensor based on titanium dioxide thick film: Enhancement of selectivity by surface coating". Applied Surface Science,. **142** , pp, 262-266,1999.